JOURNAL OF NATURAL PRODUCTS

Article

Cite This: J. Nat. Prod. 2018, 81, 1976−1983

pubs.acs.org/jnp

Flabellipparicine, a Flabelliformide-Apparicine-Type Bisindole Alkaloid from *Tabernaemontana divaricata*

You-Sheng Cai,[*,†,‡] Ariel M. Sarotti,[§] Ting-Lan Zhou,[†] Rong Huang,[†] Guofu Qiu,[†] Congkui Tian,[⊥] Ze-Hong Miao,[∥] Attila Mándi,[#] Tibor Kurtán,[#] Shugeng Cao,[*,‡] and Sheng-Ping Yang[*,†]

[†]Institute of TCM and Natural Products, School of Pharmaceutical Sciences, Wuhan University, 185 Donghu Road, Wuhan 430071, People's Republic of China

[‡]Department of Pharmaceutical Sciences, Daniel K. Inouye College of Pharmacy, University of Hawai'i at Hilo, 200 West Kawili Street, Hilo, Hawaii 96720, United States

[§]Instituto de Química Rosario (CONICET), Facultad de Ciencias Bioquímicas y Farmacéuticas, Universidad Nacional de Rosario, Suipacha 531, Rosario 2000, Argentina

[⊥]Wuling Mountain Institute of Natural Medicine, Hubei University for Nationalities, Key Laboratory of Biological Resources Protection and Utilization of Hubei Province, 39 Xueyuan Road, Enshi 445000, People's Republic of China

[∥]State Key Laboratory of Drug Research Institute of Materia Medica, Chinese Academy of Sciences, Zu Chong Zhi Road 555 Zhangjiang Hi-Tech Park, Shanghai 201203, People's Republic of China

[#]Department of Organic Chemistry, University of Debrecen, POB 400, H-4002 Debrecen, Hungary

Supporting Information

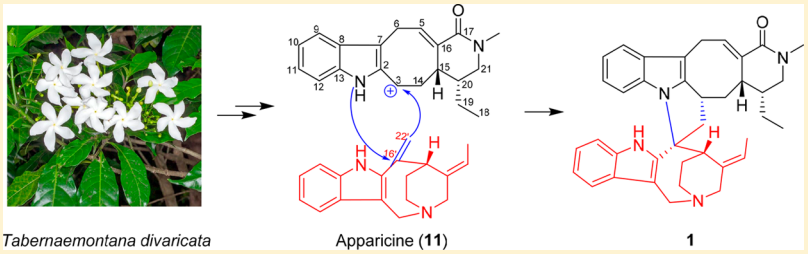

ABSTRACT: Four new monoterpenoid bisindole alkaloids, flabellipparicine (**1**), 19,20-dihydrovobparicine (**2**), 10′-demethoxy-19,20-dihydrovobatensine D (**3**), and 3′-(2-oxopropyl)ervahanine A (**4**), and 10 known monoterpenoid indole alkaloids were isolated from the stems of *Tabernaemontana divaricata*. All structures were elucidated based on spectroscopic methods, and the absolute configuration of **1** was established using conformational analysis and TDDFT-ECD calculation of selected stereoisomers. Compound **1** represents the first flabelliformide-apparicine-type bisindole alkaloid, in which the flabelliformide-like unit connects to the apparicine-like unit with a C-3−C-22′ bond and an N-1−C-16′ bond to form an uncommon five-membered ring between the two monomers. All alkaloids were evaluated for their cytotoxicity against two human cancer cell lines, MCF-7 and A-549. Compounds **2**, **4**, and **14** exhibited cytotoxicity against MCF-7 and A-549 with IC_{50} values in the range of 2 nM to 8 μM.

The monoterpenoid indole alkaloids (MIAs) are representative natural products mainly produced by plants of the Apocynaceae family. MIAs such as reserpine and vincristine have long been attractive secondary metabolites to chemists and pharmacologists due to their complex structures and prominent bioactivities.[1,2] The genus *Tabernaemontana* belonging to Apocynaceae consists of approximately 120 species, which are mainly located in the tropical and subtropical areas of Asia and Australia. About 15 species and five varieties grow in the South of China, of which many species are used as folk medicine to treat abdominal pain, headache, hypertension, scabies, and sore throat.[3] A previous chemical investigation of the genus *Tabernaemontana* generated many new monoterpenoid indole alkaloids with promising cytotoxic activities.[4−7] As a part of an ongoing search for structurally and biogenetically interesting alkaloids from the genus *Tabernaemontana*,[8] four new monoterpenoid bisindole alkaloids, flabellipparicine (**1**), having an interesting flabelliformide-apparicine-type skeleton, 19,20-dihydrovobparicine (**2**), 10′-demethoxy-19,20-dihydrovobatensine D (**3**), and 3′-(2-oxopropyl)ervahanine A (**4**), together with 10 known alkaloids, namely, tabernamine (**5**),[9] ervahanine A (**6**),[10] vobparicine (**7**),[11] 19,20-dihydrotabernamine (**8**),[12] 19,20-dihydrotabernamine A (**9**),[13] taberdivarines E (**10**),[14] (−)-apparicine (**11**),[11] tubotaiwine (**12**),[15] hydroxy-3-(2-oxopropyl)coronaridineindolenine (**13**),[16] and deoxytubulosine (**14**),[17] were isolated from *T. divaricata*. Here, the

Received: March 4, 2018
Published: August 31, 2018

DOI: 10.1021/acs.jnatprod.8b00191
J. Nat. Prod. 2018, 81, 1976−1983

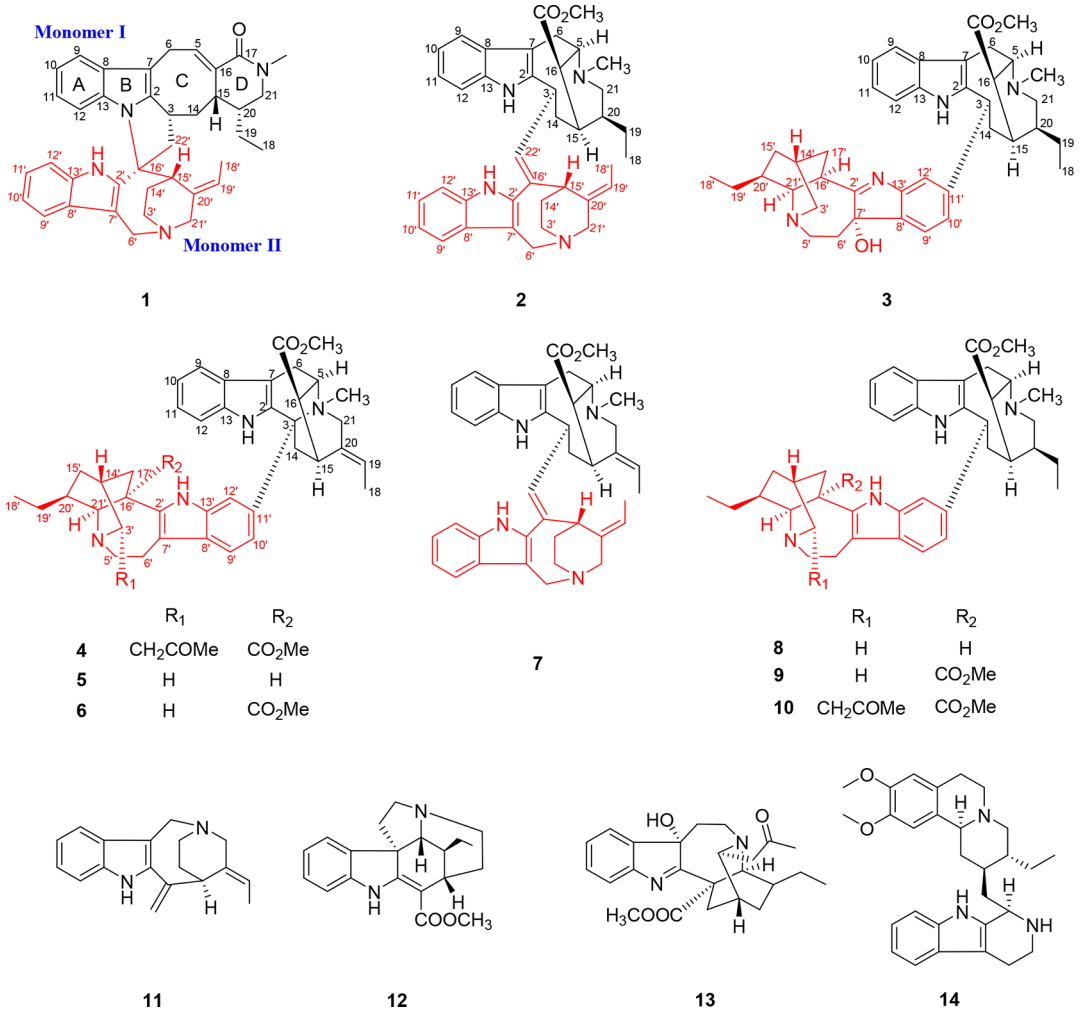

Figure 1. Compounds **1**−**14** isolated from *T. divaricata*.

isolation, structural elucidation, and the cytotoxic activity of the 14 alkaloids are discussed.

RESULTS AND DISCUSSION

Compound **1** was isolated as a light yellowish, amorphous powder. The molecular formula was determined as $C_{38}H_{42}N_4O$ (20 indices of hydrogen deficiency) by HR-ESIMS in positive mode (*m*/*z* 571.3423, calcd for $[M + H]^+$ 571.3437). Its UV spectrum displayed UV absorptions at 218.8 and 285.5 nm, typical of indole chromophores. Its IR data suggested the presence of NH (3364 cm^{-1}) and carbonyl (1713 cm^{-1}) functionalities (Figure 1). The most characteristic ^1H NMR (Table 1) signals were assigned to an indolic NH proton [δ_H 8.09 (s)], two 1,2-disubstituted benzene rings [δ_H 7.55 (d, *J* = 7.8 Hz), 7.01 (t, *J* = 7.8 Hz), 6.80 (dd, *J* = 7.8, 8.3 Hz), and 6.59 (d, *J* = 8.3 Hz); δ_H 7.51 (d, *J* = 7.9 Hz), 7.11 (dd, *J* = 7.9, 7.4 Hz), 7.18 (dd, *J* = 7.4, 7.9 Hz), and 7.24 (d, *J* = 7.4 Hz)], an *N*-methyl (δ_H 2.98, s), and two methyl groups [δ_H 1.01 (t, *J* = 7.4 Hz) and 1.72 (dd, *J* = 6.8, 1.9 Hz)]. These data showed that compound **1** was an asymmetric dimeric indole alkaloid with two unsubstituted aromatic rings, indicating an uncommon attachment between the two units, which is different from the usual vobasinyl-ibogan-type bisindole alkaloids. The chemical shifts for the *N*-methyl at 2.98 ppm, an ethyl group at 1.49 and 1.01 ppm, a double bond at 140.5 and 131.9 ppm, and an ester carbonyl at 164.5 ppm indicated the presence of an uncommon flabelliformide-like half, while the two isolated methylenes at δ_H (4.74; 4.45) and δ_H (3.86; 3.75) and an ethylidene at 1.72 and 5.65 ppm revealed the presence of an apparicine-type unit. The structures of monomeric units I and II and their connectivities were elucidated based on analysis of 2D NMR spectra (HSQC, COSY, and ^1H, ^{13}C, and $^1H-^{15}N$ HMBC) (Figure 2).

In monomeric unit I, the COSY experiment established three spin systems, C-9−C-10−C-11−C-12, C-5−C-6, and C-22′−C-3−C-14−C-15−C-20(−C-21)−C-19−C-18, as displayed (Figure 2), which was confirmed by the HMBC correlations (Figure 2). Correlation of H-5 [δ_H 7.49 (dd, *J* = 8.2, 3.5 Hz)] to C-7, C-15, and C-17, from H-14 [δ_H 1.87 (dd, *J* = 13.2, 5.0 Hz), 1.52 (m)] to C-2, C-16, and C-20, from H-6 to C-8 and C-16, and from H-3 to C-7 and C-15 revealed the presence of ring C (a cycloocta-1,4-diene moiety), which was connected to the indole moiety (rings A and B). The presence of ring D (a γ-ethyl-*N*-methyl α,β-disubstituted δ-lactam) was elucidated based on correlations of H-15 to C-17, C-19, and C-21, from the H_3-18 to C-20, from the *N*-CH_3 to C-17 and C-21, and from H_2-19 to C-21 and C-15, which was linearly aligned with the indole moiety (rings A and B) and ring C in monomeric unit I. The extended C-22′−C-3−C-14−C-15−C-20(−C-21)−C-19−C-18 spin system strongly suggested that an extra methylene group was attached to the flabelliformide unit at C-3, which was confirmed by HMBC correlations from

DOI: 10.1021/acs.jnatprod.8b00191
J. Nat. Prod. 2018, 81, 1976−1983

Table 1. ^{1}H (400 MHz) and ^{13}C NMR (100 MHz) Data for 1 and 2 in $CDCl_3$

	1		2	
position	δ_H, J (Hz)	$\delta_{C/N}$	δ_H, J (Hz)	δ_C
N-1		168.4[a]	7.59 brs	
2		141.6		136.3
3	3.69 m	39.0	4.46 m	37.8
5	7.49 dd (8.2, 3.5)	140.5	3.92 m	59.3
6	3.63 dd (13.7, 3.5); 3.45 dd (13.7, 8.2)	21.8	3.27 m; 3.02 m	17.5
7		109.9		109.7
8		132.9		130.1
9	7.55 d (7.8)	118.0	7.51 d (7.8)	117.7
10	7.01 t (7.8)	119.5	7.09 t (7.8)	119.4
11	6.80 dd (8.3, 7.8)	121.0	7.12 dd (7.8)	122.6
12	6.59 d (8.3)	112.0	7.19 d (7.8)	110.3
13		131.2		135.8
14	1.87 dd (13.2, 5.0); 1.52 m	38.4	2.59 m; 1.88 d (12.5)	36.8
15	3.36 d (8.1)	38.4	2.62, m	34.5
16		131.9	2.87 s	43.7
17		164.5		172.5
18	1.01 t (7.4)	12.0	0.96 t (7.3)	12.8
19	1.49 m	24.8	1.71 m; 1.49 m	25.7
20	1.73 m	41.4	1.40 m	43.0
21	3.62 m; 3.10 d (14.5)	49.3	3.04 m; 2.45 m	47.3
N-CH_3	2.98 s	35.6	2.53 s	43.1
CO_2CH_3			2.44 s	49.9
N-1′	8.14 brs	126.4[a]	7.81 brs	
2′		131.9		132.3
3′	3.03 m; 2.87 m	46.9	3.52 m	46.1
6′	4.74 d (17.8); 4.45 d (17.8)	53.9	4.43 d (17.6); 4.34 d (17.6)	54.3
7′		111.8		110.7
8′		127.9		128.7
9′	7.51 d (7.9)	118.3	7.37 d (7.8)	118.2
10′	7.11 dd (7.9, 7.4)	119.3	7.09 t (7.8)	119.3
11′	7.18 t (7.4)	123.1	7.13 t (7.8)	122.0
12′	7.24 d (7.4)	110.9	7.18 d (7.8)	109.9
13′		135.9		135.3
14′	2.91 m; 1.67 dd (11.4, 5.0)	27.5	2.27 m; 2.15 m	29.7
15′	3.13 d (11.4)	41.2	4.40 m	34.0
16′		70.1		137.7
18′	1.72 dd (6.8, 1.9)	13.8	1.65 d (6.6)	13.1
19′	5.65 q (6.8)	122.9	5.34 q (6.6)	119.8
20′		137.3		137.4
21′	3.86 d (15.0); 3.75 d (15.0)	55.6	3.88 d (15.2); 3.41 d (15.2)	54.56
22′	2.96 m; 2.39 dd (17.1, 6.1)	51.5	5.91 d (10.0)	133.4

[a] ^{15}N NMR data were obtained at 25 °C on an Advance 500 MHz spectrometer (Bruker) equipped with a broadband inverse probe.

H-22′ to C-2 and C-14. Therefore, the 2D structure of monomeric unit I was defined (Figure 1), with the extra C-22′ methylene a "loose end".

The ^{1}H and ^{13}C NMR data in monomeric unit II are highly similar to those in apparicine-type alkaloids, and this similarity was verified by the 2D NMR spectra analysis. The gross structure of monomeric unit II is quite similar to that of compound **11** (apparicine)[11] except for C-16′ and C-22′. The exocylic double bond [δ_H 5.39 (s), 5.26 (s); δ_C 135.6, 112.2] in apparicine was replaced by an sp^3 quaternary carbon atom (δ_C 70.1) and an sp^3 methylene (δ_C 51.5) in monomeric unit II of compound **1**. The key correlations of H-22′ to C-2 and C-14 as mentioned above and from H-22′ to C-2′ and C-15′ verified C-22′ as the first linkage between monomeric units I and II. The quaternary C-16′ was unassigned; thus, there was only one indolic NH and one more index of hydrogen deficiency, indicating a second linkage presumably from N-1 to C-16′ to form a five-membered ring.[18] The linkages were confirmed by the $^{1}H-^{15}N$ HMBC correlations from H-15′ [δ_H 3.13 (d), 11.8 Hz], H-22′ [δ_H 2.96 (m)], and H-12 [δ_H 6.59 (s)] to N-1 (δ_N 168.4) (Figure 2). Accordingly, the 2D structure of compound **1** was elucidated as shown (Figure 1).

The ($\Delta^{19'}$-*E*)-configuration was established via the NOESY correlation between H-19′ and H_2-21′. H-15 showed NOE correlations to H-3 and H-20, indicating that they were cofacial. Assuming monomeric unit I had the (3*S**, 15*R**, 20*S**) relative configuration, there should be four possible structures for **1**, (3*S**, 15*R**, 20*S**, 15′*R**, 16′*R**), (3*S**, 15*R**, 20*S**, 15′*S**, 16′*R**), (3*S**, 15*R**, 20*S**, 15′*S**, 16′*S**), and (3*S**, 15*R**, 20*S**, 15′*R**, 16′*S**).

To define the absolute configuration of **1**, the TDDFT-ECD[19,20] method was applied on the chosen (3*S*, 15*R*, 20*S*, 15′*R*, 16′*R*), (3*S*, 15*R*, 20*S*, 15′*R*, 16′*S*), (3*S*, 15*R*, 20*S*, 15′*S*, 16′*R*), and (3*S*, 15*R*, 20*S*, 15′*S*, 16′*S*) diastereomers. Preliminary Merck Molecular Force Field (MMFF) conformational searches indicated relatively low flexibility with 6−18 low-energy initial conformers. These conformers were reoptimized at the B3LYP/6-31G(d) level in vacuo and the B97D/TZVP,[21,22] the CAM-B3LYP TZVP,[23,24] and the ωB97XD[25] levels with the PCM solvent model for MeOH, and ECD calculations were performed for each set of conformers with various functionals and the TZVP basis set with the same solvent model as in the preceding step or without solvent model. Electronic circular dichroism (ECD) results of the (3*S*, 15*R*, 20*S*, 15′*R*, 16′*R*) (Figure 3) and the (3*S*, 15*R*, 20*S*, 15′*S*, 16′*R*) diastereomers showed mirror-image agreement with the experimental spectrum, while those of the (3*S*, 15*R*, 20*S*, 15′*R*, 16′*S*) and the (3*S*, 15*R*, 20*S*, 15′*S*, 16′*S*) diastereomers were similar to the experimental ones. Thus, the ECD spectrum seems to be governed mainly by the newly formed C-16′ chirality center, which determines the relative orientation of the two indole chromophores. Although the two indole moieties are expected to interact, which may give rise to exciton-coupled ECD curves, the two high-energy ECD transitions below 250 nm with opposite signs derive from many overlapping transitions, as shown by the computed rotational strengths, and without calculations this interaction is not suitable to determine the absolute configuration. Therefore, the absolute configuration of C-16′ could be obviously elucidated from the TDDFT-ECD calculations as (16′*S*). The interatomic distances of all the low-energy conformers found for each diastereoisomer were further analyzed to account for the experimentally observed NOE correlations. As depicted in Figure 4, the large distance between H-12 and H-14′ computed for the (3*S*, 15*R*, 20*S*, 15′*S*, 16′*R*) stereoisomer should not account for the NOE correlation of both protons. Similarly, the H-3/H-15′ and H-3/H-18′ NOE correlations should not be observed in the (3*S*, 15*R*, 20*S*, 15′*S*, 16′*S*) and (3*S*, 15*R*, 20*S*, 15′*R*, 16′*S*) isomers, as the calculated interatomic distances are large enough to account for the NOE enhancement experimentally observed. In contrast, the global minima structure found for (3*S*,15*R*,20*S*,15′*R*,16′*R*)-**1** matched well with the NOE correlations, with all key

DOI: 10.1021/acs.jnatprod.8b00191
J. Nat. Prod. 2018, 81, 1976−1983

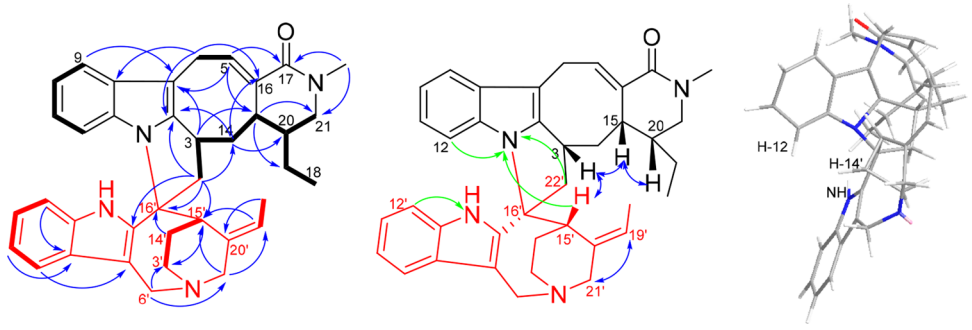

Figure 2. $^{1}H-^{1}H$ COSY (left, bold), selected HMBC (left, blue single arrows), selected $^{1}H-^{15}N$ HMBC (middle, green single arrows), and NOESY (middle and right, blue double-headed arrows) correlations of compound **1**.

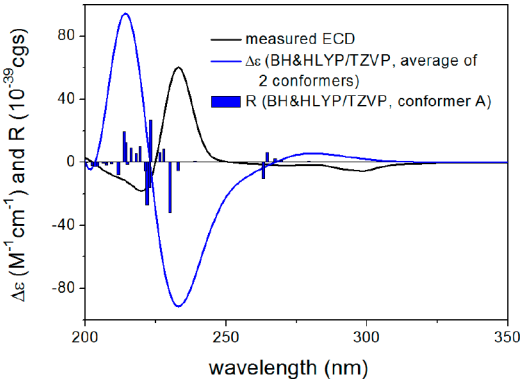

Figure 3. Comparison of the experimental ECD of **1** measured in MeOH with the BH&HLYP/TZVP PCM/MeOH spectrum of (3*S*,15*R*,20*S*,15′*R*,16′*R*)-**1** (level of optimization: CAM-B3LYP/TZVP PCM/MeOH). The bars represent the rotational strength values of the lowest-energy conformer. (The ECD spectra calculated for other isomers are provided in the SI.)

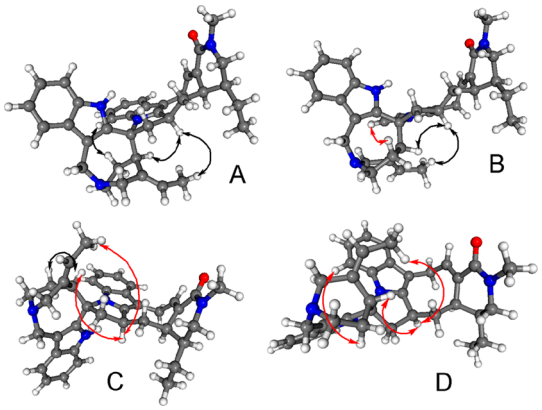

Figure 4. Lowest-energy conformers of (A) (3*S*,15*R*,20*S*,15′*R*,16′*R*)-**1**, (B) (3*S*,15*R*,20*S*,15′*S*,16′*R*)-**1**, (C) (3*S*,15*R*,20*S*,15′*S*,16′*S*)-**1**, and (D) (3*S*,15*R*,20*S*,15′*R*,16′*S*)-**1** along with feasible (black line) and nonfeasible (red line) key NOE correlations (level of optimization: CAM-B3LYP/TZVP PCM/MeOH).

interatomic distances less than 3.0 Å. These findings are also in agreement with the NMR shift calculations securing the relative configuration of **1**. As shown in the Supporting Information, the NMR calculations of the four candidate diastereoisomers (3*S*, 15*R*, 20*S*, 15′*R*, 16′*R*), (3*S*, 15*R*, 20*S*, 15′*R*, 16′*S*), (3*S*, 15*R*, 20*S*, 15′*S*, 16′*R*), and (3*S*, 15*R*, 20*S*, 15′*S*, 16′*S*) were carried out at the PCM/mPW1PW91/6-31+G**//B3LYP/6-31G* level of theory, as recommended for DP4+ analysis.[26] As expected, the isomer featuring the (3*S*, 15*R*, 20*S*, 15′*R*, 16′*R*) relative configuration displayed the closest match between experimental and computed NMR shifts. The CMAE (corrected mean absolute error, defined as $\sum_n|\delta_{sc} - \delta_{exp}|/n$) computed for the (3*S*, 15*R*, 20*S*, 15′*R*, 16′*R*) isomer was 2.2 ppm (^{13}C NMR data) and 0.13 ppm (^{1}H NMR data), lower than the corresponding values obtained for the remaining three isomers (2.3−2.6 and 0.19−0.21 ppm for carbon and proton data, respectively). As a result, the DP4+ probability strongly supported the most likely relative configuration of **1** as (3*S*, 15*R*, 20*S*, 15′*R*, 16′*R*) in high confidence (>99.9%). Therefore, with the information provided by the ECD and NMR calculations, the absolute configuration of **1** was defined as (3*R*, 15*S*, 20*R*, 15′*S*, 16′*S*).

Compound **2** was obtained as a light yellow, amorphous solid with the molecular formula $C_{39}H_{46}N_4O_2$ based on the HR-ESIMS positive ion ($[M + H]^+$ at m/z 603.3699). Comparison of the 1D and 2D NMR data of **2** (Table 1) with those of vobparicine (**7**)[11] suggested the 2D structures of **2** and **7** were similar, except that the ethylene group was replaced by an ethyl group in **2**. The molecular formula of **7**, $C_{39}H_{44}N_4O_2$, is two units less than that of **2**, confirming that **2** was a reduced product of **7**. The configurations at C-3, C-5, C-15, and C-15′ were deduced to be the same as in **7** by the similarity of the 1D and 2D NMR data of **2** and **7**, along with biosynthetic considerations. The NOESY correlations of H-20/H-14 and H-20/H-15 suggested the C-20 ethyl side chain is β-oriented to the ring system. Hence, the structure of **2** was determined to be 19,20-dihydrovobparicine (Figure 1).

Compound **3** was obtained as a light yellowish solid with $[\alpha]_D^{20}$ +10 (*c* 0.1, MeOH). Its UV spectrum displayed absorption maxima at 293, 286, and 228 nm, suggesting an indole chromophore, while its IR absorptions implied the presence of NH/OH (3358 cm^{-1}) and ester carbonyl functions (1721 cm^{-1}). A molecular formula of $C_{40}H_{50}N_4O_3$ was deduced from HR-ESIMS (m/z 635.3966, calcd for $[M + H]^+$ 635.3961). An analysis of the ^{1}H NMR (Table 2) data revealed only one indolic NH at δ_H 7.56. The rest of the ^{1}H NMR signals indicated an unsubstituted indole ring (δ_H 7.01, 7.02, 7.05, and 7.53), another indole moiety substituted at C-11′ (δ_H 7.01, 7.20, and 7.30), a methoxy (δ_H 2.43), an *N*-Me (δ_H 2.53), and two ethyl groups at δ_H 0.95, 1.72 and δ_H 0.93, 1.81, respectively. The absence of the indole NH′ in the iboga half, connected to an imine carbon (δ_C 194.3, C-2′), together with an oxygenated sp^3 tertiary carbon atom (δ_C 87.4, C-7′), implied that the structural skeleton of the iboga moiety is similar to the compound hydroxy-3-(2-oxopropyl)-coronaridineindolenine (**13**).[16] Detailed analysis of the 2D

DOI: 10.1021/acs.jnatprod.8b00191
J. Nat. Prod. 2018, 81, 1976−1983

Table 2. ^{1}H (400 MHz) and ^{13}C NMR (100 MHz) Data for 3 and 4 in $CDCl_3$

	3		4	
position	δ_H, J (Hz)	δ_C	δ_H, J (Hz)	δ_C
N-1	7.56		7.45 brs	
2		136.5		136.8
3	4.51 dd (3.0, 12.7)	45.2	4.67 d (10.0)	45.3
5	3.97 t (7.74)	59.4	4.07 m	59.8
6	3.10 m; 3.40 m	17.5	3.52 m; 3.27 m	19.4
7		110.5		110.4
8		129.8		129.8
9	7.53 dd (8.0, 2.0)	117.7	7.59 m	117.6
10	7.05 m	118.9	7.01 dd (8.0)	119.5
11	7.02 m	121.6	7.08 m	121.7
12	7.01 d (7.8)	109.9	7.02 d (8.2)	109.9
13		136.1		137.3
14	1.93 m; 2.53 m	41.2	1.25 m	38.9
15	2.61 m	34.6	3.80 m	33.6
16	3.00 m	43.7	2.75 s	47.1
17		172.6		171.9
18	0.95 t (7.2)	12.9	1.69 d (6.1)	12.4
19	1.72 m	25.7	5.35 d (7.0)	118.9
20	2.53 m	43.0		137.6
21	3.00 m; 3.05 m	47.1	3.79 m; 2.93 m	52.4
N-CH_3	2.53	42.95	2.49 s	49.9
CO_2CH_3	2.43	49.93	2.11 s	42.4
N-1′			7.66 brs	
2′		194.3		136.0
3′	3.46 m; 2.98 m	49.1	3.29 m	55.4
5′	2.67 m; 2.78 m	49.4	3.13 m	51.4
6′	1.11 m; 1.72 m	31.8	3.17 m; 2.95 m	22.1
7′		87.4		110.1
8′		140.1		127.5
9′	7.20 d (7.6)	121.3	7.39 d (8.0)	118.7
10′	7.01 d (7.6)	125.1	7.08 d (8.0)	119.0
11′		152.6		140.0
12′	7.30 s	119.8	7.03 s	109.4
13′		148.2		135.8
14′	1.48 m	27.1	1.68 m	30.8
15′	1.87 m	32.2	1.60 m; 1.44 m	27.0
16′	1.46 m	40.4		54.7
17′	2.10 m; 2.17 m	33.8	2.60 m; 1.90 m	37.6
18′	0.93 t (7.4)	11.8	0.91 t (7.6)	11.7
19′	1.81 m	27.2	1.44 m	26.8
20′	2.87 m	43.6	1.25 m	38.4
21′	3.51 s	53.4	3.58 s	58.0
22′			2.75 m	46.6
23′				208.6
24′			2.20 s	31.0
CO_2CH_3				175.3
CO_2CH_3			3.70 s	52.6

NMR data suggested that **3** had the same skeleton as vobatensine D,[27] except that the double bond $\Delta^{19(20)}$ and the aromatic methoxy group at C-10′ in vobatensine D were absent in **3**. Meanwhile, an additional sp^3 methylene group (H_2-19) was present, and its orientation was determined by NMR data and biosynthetic considerations. As in the case of known compound 19,20-dihydrotabernamine (**8**),[12] the NMR data suggested similar configurations at C-3 (α-substitution), C-16, and C-20 of the vobasinyl unit and at C-14′, C-16′, C-20′, and C-21′ of the iboga unit (Figure 1). The α-orientation of 7′-OH was determined based on the biosynthetic pathway, since the C-7 configuration of 7-hydroxyindolenine of ibogaine has been previously established.[28] Thus, the structure of **3** was established to be 10′-demethoxy-19,20-dihydrovobatensine D as shown (Figure 1).

Compound **4** was isolated as a light yellowish solid with the molecular formula $C_{45}H_{54}N_4O_5$, determined by the HR-ESIMS ion ($[M + H]^+$ at m/z = 731.4173). Detailed comparison of the 1D and 2D NMR data (Table 2) of **4** with those of **6** (ervahanine A)[10] indicated similar structures, except for the 2-oxopropyl substituent at C-3′ in the iboga moiety of **4**. The configurations of **4** were determined to be the same as ervahanine A (**6**)[10] and taberdivarines E (**10**)[14] by NMR data and biosynthetic considerations. Accordingly, the structure of **4** was elucidated to be 3′-(2-oxopropyl)ervahanine A.

Among the four new compounds, the structure of compound **1** is unique because monomeric unit I (featuring four rings [6 + 5 + 8 + 6] linearly aligned) is uncommon in nature. Similar to flabelloformides A and B,[18,29] monomeric unit I could be biosynthetically derived from vobasinol[30] (Scheme 1). Starting from vobasinol, from which 19,20-dihydrovobparicine (**2**) would be generated, a β-elimination leads to a tricyclic keto ester, which on attack by the secondary amine nitrogen (N-4) on the ester carbonyl, followed by elimination of MeOH, gives the tetracyclic lactam incorporating the flabelliformide[29] ring system. The (15′*S*) absolute configuration of **1** is in accordance with the (15*S*) configuration of (−)-apparicine (**11**),[11] the biosynthetic precursor of monomeric unit II. After formation of a C-3 carbocation by removal of the C-3 hydroxy group, the electrophilic addition of C-3 to C-22′ of the exocyclic double bond, followed by nucleophilic addition of the nitrogen (N-1) to C-16′, would generate compound **1**.

All the monoterpenoid indole alkaloids isolated form *T. divaricata* were evaluated against the human breast (MCF-7) and human lung (A-549) cancer cell lines. Bisindole alkaloids **1**−**10** and **14** were active in a range of 2 nM to 8.1 μM (Table 3); however, monoterpenoid indole monomers **11**−**13** were inactive. Alkaloids **2**, **4**−**7**, and **10**, having two indolic NH groups, displayed a similar cytotoxicity against MCF-7 and A-549, whereas **1** and **3**, having just one indolic NH group, showed much less inhibitory activity toward these two cell lines. Compared to the monoterpenoid indole alkaloids, the β-carbolinebenzoquinolizidine alkaloid deoxytubulosine (**14**) showed potent inhibitory effects toward MCF-7 and A-549 with IC_{50} values of 2 and 87 nM (Table 3), respectively. The bioassay results suggested that the indolic NH group plays an important role in bisindole alkaloids for the cytotoxicity, while the β-carbolinebenzoquinolizidine alkaloid was much more cytotoxic than monoterpenoid indole alkaloids.

EXPERIMENTAL SECTION

General Experimental Procedures. Optical rotations were measured using a PerkinElmer model 341 polarimeter. ECD spectra were recorded on a JASCO J-810 spectropolarimeter. UV absorption spectra were measured using a Shimadzu UV-1700 spectrophotometer. IR spectra were recorded on a Thermo Nexus470 FT-IR spectrometer. NMR spectra were acquired using a BIOSPIN AV 400 NMR instrument (Bruker) at 400 MHz for ^{1}H NMR and 100 MHz for ^{13}C NMR. $^{1}H-^{15}N$ HMBC data were obtained at 25 °C on an Advance 500 MHz spectrometer (Bruker) equipped with a broadband inverse probe. HR-ESIMS data were obtained on an LTQ Orbitrap XL mass instrument (ThermoFisher). Column chromatography (CC) was performed with silica gel (200−300 mesh, Anhui Liangchen

DOI: 10.1021/acs.jnatprod.8b00191
J. Nat. Prod. 2018, 81, 1976−1983

Scheme 1. Proposed Biosynthetic Pathway for Compounds 1 and 2

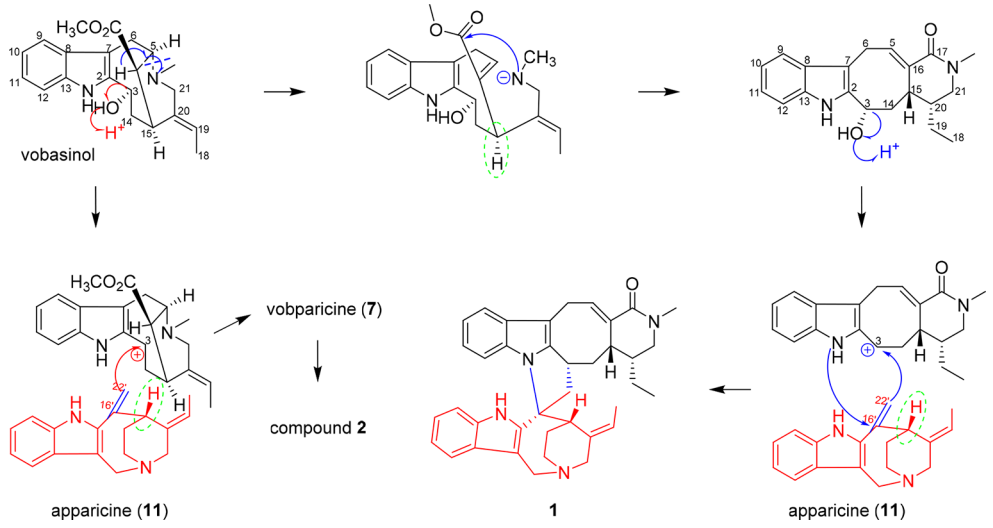

Table 3. Cytotoxic Activity of 1−10 and 14 (IC_{50}, μM)

compound	IC_{50} (μM)	
	MCF-7	A-549
1	>10 μM	7.5
2	0.8	8.1
3	1.3	>10 μM
4	2.8	1.2
5	1.3	3.2
6	7.3	1.2
7	1.3	4.0
9	5.4	>10 μM
10	1.3	1.2
14	0.002	0.09
SN38[a]	<0.1 nM	0.2

[a]SN38 (7-ethyl-10-hydroxycamptothecin) was used as positive control.

Guiyuan Material Ltd., Anhui, China). Size-exclusion chromatography was performed with Sephadex LH-20 (Pharmacia, Sweden).

Plant Material. A specimen of *T. divaricata* was collected from Xishuangbanna, Yunnan Province, People's Republic of China, in July 2013 and identified by Mr. Jing-Yun Cui of the Xishuangbanna Tropical Botanical Garden, Chinese Academy of Sciences. A voucher specimen (WHU20130821) is available for inspection at the Institute of TCM & Natural Products, School of Pharmaceutical Sciences, Wuhan University.

Extraction and Isolation. The stems of *T. divaricata* were pulverized to a powder after desiccation. The powder (6 kg) was exhaustively extracted (3 × 7 days) with 95% EtOH (3 × 10 L) to give the crude (71 g), which was dissolved in 1.5 L of acidified water (adjusted to pH 1−2 using 10% H_2SO_4). After removal of the nonalkaloids by extracting with EtOAc (1.0 L × 3), the acidic aqueous phase was basified with Na_2CO_3 to pH 8−9 and partitioned with $CHCl_3$ (1.5 L × 3) to afford the crude alkaloids (10.2 g), which were subsequently chromatographed over silica gel eluted with CH_2Cl_2/MeOH/Et_2NH (50:1:0.1 to 1:1:0.1) into three fractions (G1−G3).

G1 (6.1 g) was chromatographed over silica gel (CH_2Cl_2/MeOH/Et_2NH, 50:1:0.1 to 1:1:0.1) to afford six subfractions, G1a−G1f. G1a (2.13 g) was purified by silica gel CC eluted with petroleum ether/EtOAc/Et_2NH (5:1:0.1 to 3:1:0.1) to generate two major fractions. One fraction was purified by silica gel CC with petroleum ether/EtOAc/Et_2NH, 5:1:0.1, to afford **8** (168 mg) and **14** (10 mg), and the second fraction with petroleum ether/2-propanol/Et_2NH, 7.5:1:0.1, to provide **9** (159 mg) and **3** (27 mg). G1b (2.25 g) was further purified on silica gel CC with petroleum ether/EtOAc/Et_2NH (5:1:0.1 to 3:1:0.1) to give three subfractions, G1b1, G1b2, and G1b3. G1b1 was purified over silica gel CC (petroleum ether/EtOAc/Et_2NH, 5:1:0.2) to give **10** (78 mg), G1b2 was subjected to silica gel CC (petroleum ether/EtOAc/Et_2NH, 5:1:0.4) to give **5** (316 mg), and G1b3 was purified with petroleum ether/EtOAc/Et_2NH, 4:1:0.2, to afford **6** (38 mg). G1c (1.2 g) was isolated by silica gel column chromatography to afford **4** (36 mg) and **1** (10 mg) (eluted with petroleum ether/EtOAc/Et_2NH, 5:1:0.2).

G2 (2.1 g) was chromatographed over silica gel to afford two major components. One fraction was separated and purified to give **11** (105 mg) over silica gel CC with petroleum ether/EtOAc/Et_2NH, 5:1:0.1, and the second one was further separated by silica gel to afford **12** (36 mg) and **13** (21 mg).

G3 (1.8 g) was separated and purified over silica gel CC (petroleum ether/EtOAc/Et_2NH, 3.5:1:0.1) to give **2** (17 mg) and **7** (10 mg).

*Flabellipparicine (**1**):* $[\alpha]_D^{20}$ +28 (*c* 0.1, $CHCl_3$); UV (MeOH) λ_{max} (log ε) 285.5 (4.26), 244.5 (4.36), 218.8 (3.67) nm; ECD {MeOH, λ [nm] ($\Delta\varepsilon$), *c* 0.1 × 10^{-4} M} 298 (−5.49), 271sh (−2.01), 233 (+60.40), 220 (−18.16), 210sh (−8.60); IR (KBr) ν_{max} 3364, 2922, 2856, 1713, 1657, 1461, 1384, 741 cm^{-1}; ^1H and ^{13}C NMR data ($CDCl_3$), see Table 1; HR-ESIMS *m*/*z* 571.3423 $[M + H]^+$ (calcd for $C_{38}H_{43}N_4O$, 571.3437).

*19,20-Dihydrovobparicine (**2**):* $[\alpha]_D^{20}$ +26 (*c* 0.1, MeOH); UV (MeOH) λ_{max} (log ε) 295 (4.22), 239 (4.29), 234 (4.28) nm; IR (KBr) ν_{max} 3417, 2925, 2854, 1723, 1660, 1462, 1384, 1228, 1155, 1060, 741 cm^{-1}; ^1H and ^{13}C NMR data ($CDCl_3$), see Table 1; HR-ESIMS *m*/*z* 603.3690 $[M + H]^+$ (calcd for $C_{39}H_{47}N_4O_2$, 603.3699).

*10′-Demethoxy-19,20-dihydrovobatensine D (**3**):* $[\alpha]_D^{20}$ +10 (*c* 0.1, MeOH); UV (MeOH) λ_{max} (logε) 293 (4.01), 286 (4.05), 228 (4.62) nm; IR (KBr) ν_{max} 3358, 2927, 2866, 1721, 1561, 1459, 1314, 1102, 1062, 1010, 742 cm^{-1}; 1D NMR data, see Table 2; HR-ESIMS *m*/*z* 635.3966 $[M + H]^+$ (calcd for $C_{40}H_{51}N_4O_3$ 635.3961).

*3′-(2-Oxopropyl)ervahanine A (**4**):* $[\alpha]_D^{20}$ −90 (*c* 0.1, MeOH); UV (MeOH) λ_{max} (log ε) 288 (4.2), 231 (4.68) nm; IR (KBr) ν_{max} 3390, 2928, 2868, 1710, 1650, 1459, 1337, 1222 cm^{-1}; 1D NMR data, see Table 2; HR-ESIMS *m*/*z* 731.4161 $[M + H]^+$ (calcd for $C_{45}H_{55}N_4O_5$, 731.4173).

Computational Section. Mixed torsional/low-frequency mode conformational searches were carried out by means of the Macromodel 10.8.011 software using the MMFF with an implicit solvent model for chloroform.[31] Geometry reoptimizations were carried out at the B3LYP/6-31G(d) level in vacuo, the B97D/TZVP,[20,21] the CAM-B3LYP/TZVP,[22,23] and the ωB97XD[25] levels with the PCM solvent model for MeOH. TDDFT-ECD calculations were carried out using various functionals (B3LYP, BH&HLYP,

DOI: 10.1021/acs.jnatprod.8b00191
J. Nat. Prod. 2018, 81, 1976−1983

CAM-B3LYP, PBE0) and the TZVP basis set as implemented in the Gaussian 09 package with the same or no solvent model as in the preceding DFT optimization step.[32] ECD spectra were produced as sums of Gaussians with 3000 cm^{-1} widths at half-height (corresponding to ca. 16 at 230 nm), using dipole-velocity-computed rotational strength values.[33] Boltzmann distributions were evaluated based on the ZPVE-corrected B3LYP energies in the gas-phase calculations and the uncorrected B97D/TZVP and CAM-B3LYP/TZVP energies in the PCM ones. The NMR calculations were carried out at the PCM/mPW1PW91/6-31+G**//B3LYP/6-31G* level of theory using the GIAO method,[34] with $CHCl_3$ as solvent. The unscaled chemical shifts (δ_u) were calculated using tetramethylsilane (TMS) as reference standard according to $\delta_u = \sigma_0 - \sigma_x$, where σ_x is the Boltzmann-averaged shielding tensor (over all significantly populated conformations) and σ_0 is the shielding tensor of TMS calculated at the same level of theory employed for σ_x. The scaled chemical shifts (δ_s) were calculated as $\delta_s = (\delta_u - b)/m$, where m and b are the slope and intercept, respectively, deduced from a linear regression calculation on a plot of δ_u against δ_{exp}. The DP4+ calculations were run by the Excel spreadsheet available for free at sarotti-nmr.weebly.com or as part of the Supporting Information of the original paper.[26] The MOLEKEL software package was used for visualization of the results.[35]

Antiproliferative Assays. The antiproliferative activities of all the alkaloids were tested against MCF-7 human breast adenocarcinoma and A-549 human lung carcinoma cell lines. The concentration giving 50% inhibition of cell growth (IC_{50}) was calculated according to the procedure described in the literature.[8]

■ ASSOCIATED CONTENT

Supporting Information

The Supporting Information is available free of charge on the ACS Publications website at DOI: 10.1021/acs.jnatprod.8b00191.

1D and 2D NMR of **1**−**4** and **7** in $CDCl_3$; $^1H-^{15}N$ HMBC of **1** in $CDCl_3$; ^1H and ^{13}C NMR of **5** in $CDCl_3$; ^1H NMR of **6** in $CDCl_3$ (PDF)

■ AUTHOR INFORMATION

Corresponding Authors

*Tel (Y.-S. Cai): +86-156-23752985. E-mail: cysh2002@whu.edu.cn.

*Tel (S. Cao): +1-808-9818017. E-mail: scao@hawaii.edu.

*Tel (S.-P. Yang): +86-187-21307490. E-mail: sp-yang@126.com.

ORCID

You-Sheng Cai: 0000-0001-9325-0241

Ariel M. Sarotti: 0000-0002-8151-0306

Attila Mándi: 0000-0002-7867-7084

Tibor Kurtán: 0000-0002-8831-8499

Shugeng Cao: 0000-0001-6684-8221

Notes

The authors declare no competing financial interest.

■ ACKNOWLEDGMENTS

Financial support for this work from the National Natural Science Foundation of China (No. 21402146), the National Key R & D Program of China (No. 2018YFC0311002), the Natural Science Foundation of Hubei Province (No. 2015CFB421), and the open project of Hubei Key Laboratory of Purification and Application of Plant Anti-Cancer Ingredients (No. HLPAI2014001) is gratefully acknowledged. We are grateful to the EU and the European Regional Development Fund under Project GINOP-2.3.2-15-2016-00008 for their financial support of the ECD calculations and the Governmental Information-Technology Development Agency (KIFÜ) for CPU time. The authors are grateful to H. Liu from State Key Laboratory of Magnetic Resonance and Molecular and Atomic Physics, Wuhan Institute of Physics and Mathematics, CAS, for her help in carrying out $^1H-^{15}N$ HMBC experiments.

■ REFERENCES

(1) Dewick, P. M. *Alkaloids. Medicinal Natural Products: A Biosynthetic Approach*, 3rd ed.; John Wiley & Sons Ltd.: Chichester, 2009; pp 369−380.

(2) Cai, X. H.; Bao, M. F.; Zhang, Y.; Zeng, C. X.; Liu, Y. P.; Luo, X. D. *Org. Lett.* **2011**, *13*, 3568−3571.

(3) Li, P. T.; Leeuwenberg, A. J. M.; Middleton, D. J. *Flora of China*; Science Press: Beijing, 1995; Vol. *16*, pp 152−153.

(4) Zhang, Y.; Yuan, Y.-X.; Goto, M.; Guo, L.-L.; Li, X.-N.; Morris-Natschke, S. L.; Lee, K.-H.; Hao, X.-J. *J. Nat. Prod.* **2018**, *81*, 562−571.

(5) Low, Y. Y.; Lim, K. H.; Choo, Y. M.; Pang, H. S.; Kam, T. S. *Tetrahedron Lett.* **2010**, *51*, 269−272.

(6) Kazumasa, Z.; Tomoko, H.; Takahiro, H.; Yusuke, H.; Koichi-ro, K.; Abdul, R.; Idha, K.; Noor, C. Z.; Motoo, S.; Hiroshi, M. *J. Nat. Prod.* **2009**, *72*, 1686−1690.

(7) Kam, T.-S.; Sim, K.-M.; Pang, H.-S.; Koyano, T.; Hayashic, M.; Komiyama, K. *Bioorg. Med. Chem. Lett.* **2004**, *14*, 4487−4489.

(8) Zhou, S.-Y.; Zhou, T.-L.; Qiu, G.; Huan, X.; Miao, Z.-H.; Yang, S.-P.; Cao, S.; Fan, F.; Cai, Y.-S. *Planta Med.* **2018**, DOI: 10.1055/a-0608-4988.

(9) Kingston, D. G.; Gerhart, B. B.; Ionescu, F.; Mangino, M. M.; Sami, S. M. *J. Pharm. Sci.* **1978**, *67*, 249−251.

(10) Feng, X. Z.; Kan, C.; Husson, H. P.; Potier, P.; Kan, S. K.; Lounasmaa, M. *J. Nat. Prod.* **1981**, *44*, 670−675.

(11) Van Beek, T. A.; Verpoorte, R.; Svendsen, A. B. *Tetrahedron Lett.* **1984**, *25*, 2057−2060.

(12) Ingkaninan, K.; Changwijit, K.; Suwanborirux, K. *J. Pharm. Pharmacol.* **2006**, *58*, 847−852.

(13) Henriques, A. T.; Melo, A. A.; Moreno, P. R. H.; Ene, L. L.; Henriques, J. A. P.; Schapoval, E. E. S. *J. Ethnopharmacol.* **1996**, *50*, 19−25.

(14) Zhang, B.-J.; Teng, X.-F.; Bao, M.-F.; Zhong, X.-H.; Ni, L.; Cai, X.-H. *Phytochemistry* **2015**, *120*, 46−52.

(15) Yamauchi, T.; Abe, F.; Padolina, W. G.; Dayrit, F. M. *Phytochemistry* **1990**, *29*, 3321−3325.

(16) Huang, J. P.; Feng, Z. M.; Zheng, C. F.; Zhang, P. C.; Ma, Y. M. *Chin. Chem. Lett.* **2006**, *17*, 779−782.

(17) Monteiro, H.; Budzikiewicz, H.; Djerassi, C.; Arndt, R. R.; Baarschers, W. H. *Chem. Commun.* **1965**, *14*, 317−318.

(18) Van Beek, T. A.; Lankhorst, P. P.; Verpoorte, R.; Massiot, G.; Fokkens, R.; Erkelens, C.; Perera, P.; Tibell, C. Z. *Z. Naturforsch., B: J. Chem. Sci.* **1985**, *40b*, 693−701.

(19) Pescitelli, G.; Bruhn, T. *Chirality* **2016**, *28*, 466−474.

(20) Mándi, A.; Mudianta, I. W.; Kurtán, T.; Garson, M. J. *J. Nat. Prod.* **2015**, *78*, 2051−2056.

(21) Grimme, S. *J. Comput. Chem.* **2006**, *27*, 1787−1799.

(22) Sun, P.; Xu, D. X.; Mándi, A.; Kurtán, T.; Li, T. J.; Schulz, B.; Zhang, W. *J. Org. Chem.* **2013**, *78*, 7030−7047.

(23) Yanai, T.; Tew, D. P.; Handy, N. C. *Chem. Phys. Lett.* **2004**, *393*, 51−57.

(24) Sun, Y. Z.; Kurtán, T.; Mándi, A.; Tang, H.; Chou, Y.; Soong, K.; Su, L.; Sun, P.; Zhuang, C. L.; Zhang, W. *J. Nat. Prod.* **2017**, *80*, 2930−2940.

(25) Chai, J. D.; Head-Gordon, M. *Phys. Chem. Chem. Phys.* **2008**, *10*, 6615−6620.

(26) Grimblat, N.; Zanardi, M. M.; Sarotti, A. M. *J. Org. Chem.* **2015**, *80*, 12526−12534.

(27) Sim, D. S.-Y.; Teoh, W.-Y.; Sim, K.-S.; Lim, S.-H.; Thomas, N. F.; Low, Y.-Y.; Kam, T.-S. *J. Nat. Prod.* **2016**, *79*, 1048−1055.

DOI: 10.1021/acs.jnatprod.8b00191
J. Nat. Prod. 2018, 81, 1976−1983

(28) Madinaveitia, A.; De la Fuente, G.; Gonzalez, A. *Helv. Chim. Acta* **1998**, *81*, 1645−1653.
(29) Liang, S.; Chen, H.-S.; Shen, Y.-H.; Jin, L.; Zhang, W.-D. *Helv. Chim. Acta* **2007**, *90*, 1467−1470.
(30) Van der Heijiden, R.; Louwe, C. L.; Verhey, E. R.; Harkes, P. A.; Verpoorte, R. *Planta Med.* **1989**, *55*, 158−162.
(31) *MacroModel*; Schrödinger, LLC, 2015, http://www.schrodinger.com/MacroModel.
(32) Frisch, M. J.; Trucks, G. W.; Schlegel, H. B.; Scuseria, G. E.; Robb, M. A.; Cheeseman, J. R.; Scalmani, G.; Barone, V.; Mennucci, B.; Petersson, G. A.; Nakatsuji, H.; Caricato, M.; Li, X.; Hratchian, H. P.; Izmaylov, A. F.; Bloino, J.; Zheng, G.; Sonnenberg, J. L.; Hada, M.; Ehara, M.; Toyota, K.; Fukuda, R.; Hasegawa, J.; Ishida, M.; Nakajima, T.; Honda, Y.; Kitao, O.; Nakai, H.; Vreven, T.; Montgomery, J. A., Jr.; Peralta, J. E.; Ogliaro, F.; Bearpark, M.; Heyd, J. J.; Brothers, E.; Kudin, K. N.; Staroverov, V. N.; Kobayashi, R.; Normand, J.; Raghavachari, K.; Rendell, A.; Burant, J. C.; Iyengar, S. S.; Tomasi, J.; Cossi, M.; Rega, N.; Millam, J. M.; Klene, M.; Knox, J. E.; Cross, J. B.; Bakken, V.; Adamo, C.; Jaramillo, J.; Gomperts, R.; Stratmann, R. E.; Yazyev, O.; Austin, A. J.; Cammi, R.; Pomelli, C.; Ochterski, J. W.; Martin, R. L.; Morokuma, K.; Zakrzewski, V. G.; Voth, G. A.; Salvador, P.; Dannenberg, J. J.; Dapprich, S.; Daniels, A. D.; Farkas, Ö.; Foresman, J. B.; Ortiz, J. V.; Cioslowski, J.; Fox, D. J. *Gaussian 09*, Revision E. 01; Gaussian: Wallingford, CT, USA, 2013.
(33) Stephens, P. J.; Harada, N. *Chirality* **2010**, *22*, 229−233.
(34) (a) Ditchfield, R. *J. Chem. Phys.* **1972**, *56*, 5688−5691. (b) Ditchfield, R. *Mol. Phys.* **1974**, *27*, 789−807. (c) Rohlfing, C. M.; Allen, L. C.; Ditchfield, R. *Chem. Phys.* **1984**, *87*, 9−15. (d) Wolinski, K.; Hinton, J. F.; Pulay, P. *J. Am. Chem. Soc.* **1990**, *112*, 8251−8260.
(35) Varetto, U. M. *MOLEKEL*; Swiss National Supercomputing Centre: Manno, Switzerland, 2009.

DOI: 10.1021/acs.jnatprod.8b00191
J. Nat. Prod. 2018, 81, 1976−1983